CRYSTAL GROWTH & DESIGN

Article

pubs.acs.org/crystal

Absolute Configuration and Polymorphism of 2-Phenylbutyramide and α-Methyl-α-phenylsuccinimide

Published as part of the Crystal Growth & Design Mikhail Antipin Memorial virtual special issue

Victor N. Khrustalev,[†,‡] Bhupinder Sandhu,[†] Samuel Bentum,[†] Alexandr Fonari,[†] Arcadius V. Krivoshein,*[,†,§] and Tatiana V. Timofeeva*[,†]

[†]Department of Biology & Chemistry, New Mexico Highlands University, 803 University Avenue, Las Vegas, New Mexico 87701, United States

[‡]A. N. Nesmeyanov Institute of Organoelement Compounds, Russian Academy of Sciences, 28 Vavilov Street, B-334, Moscow 119991, Russian Federation

[§]Department of Basic & Social Sciences, Albany College of Pharmacy and Health Sciences, 106 New Scotland Avenue, Albany, New York 12208, United States

Supporting Information

ABSTRACT: Crystal structures of racemic and homochiral forms of 2-phenylbutyramide (**1**) and 3-methyl-3-phenylpyrrolidine-2,5-dione (**2**) were investigated in detail by a single crystal X-ray diffraction study. Absolute configurations of the homochiral forms of **1** and **2**, obtained by chromatographic separation of racemates, were determined. It was revealed that racemate and homochiral forms of **1** are very similar in terms of supramolecular organization (H-bonded ribbons) in crystal, infrared (IR) spectral characteristics, and melting points. The presence of two different molecular conformations in homochiral forms of **1** allowed mimicking of crystal packing of the H-bonded ribbons in racemate **1**. Two polymorph modifications (monoclinic and orthorhombic) comprising very similar H-bonded *zigzag*-like chains were found for the homochiral forms of compound **2** that were significantly different in terms of crystal structure, IR spectra, and melting points from the racemic form of **2**. Unlike compound **1**, homochiral forms of compound **2** have a higher density than the corresponding racemate which contradicts the Wallach rule and indicates that, in this case, homochiral forms are more stable than racemate forms.

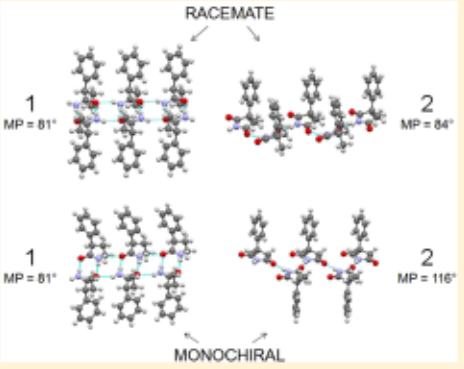

INTRODUCTION

It is universally recognized that shape of a molecule, or a molecule's spatial structure, plays a key role in determining its physiological and pharmacological properties. The chiral nature of all living organisms suggests that the most suitable forms of drugs for organisms might be not the racemic form of an active compound (a mixture of equal quantities of two molecules that are mirror images of one another) but rather one of its chiral forms. Significant attention to this problem was raised by the thalidomide tragedy in late 50s to early 60s of the 20th century, when the racemic form of thalidomide was marketed as a sedative and antinausea treatment for pregnant women. Soon after the beginning of thalidomide usage, it was found that this drug produced embryotoxic and teratogenic effects.[1−3] At that time, these effects were believed to be related to only one form of thalidomide, its (*S*)-(−)-enantiomer.[4] However, since thalidomide undergoes fast racemization under physiological conditions,[5] administration of only the (*R*)-(+)-enantiomer most probably would not help to avoid those tragic consequences. Nevertheless, these events attracted significant attention to the separation of enantiomers, testing of their bioactivity, and estimation of their absolute configuration using X-ray diffraction method.[6,7]

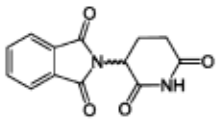

Thalidomide, *(RS)*-2-(2,6-dioxopiperidin-3-yl)-1*H*-isoindole-1,3(2*H*)-dione

Recently, the attention of our research groups was aroused toward crystallographic studies of compounds with anticonvulsant activity. The thalidomide story and examples of stereoselective pharmacological activity clearly demonstrate that enantiomeric composition and relation of molecular absolute configuration to its bioactivity need to be taken into account for all established or prospective chiral pharmaceuticals.

Received: February 25, 2014
Revised: May 19, 2014
Published: June 5, 2014

We have recently discovered that α-substituted lactams, succinimides, and carboxamides inhibit the function of the neuronal acetylcholine receptor (nAChR) *in vitro* with a potency that correlates with their ability to prevent maximal electroshock (MES)-induced seizures *in vivo*.[8] One of the simplest compounds that inhibit the receptor is 2-phenylbutyramide (**1**, Scheme 1). It shows promising antiepileptic activity in several rodent models of epilepsy.[8] Another compound that inhibits the receptor is α-methyl-α-phenylsuccinimide (**2**, Scheme 1), which is the pharmacologically active, N-demethylated metabolite of a well-known antiepileptic drug methsuximide.[9] Methsuximide marketed under the trade name of Celontin by Pfizer and is considered to be a safe and effective antiepileptic drug.[10,11] Both **1** and **2** are chiral, and we recently reported chromatographic resolution and pharmacological testing of (+) and (−) enantiomers of these drugs.[12] To the best of our knowledge, no polymorphic modifications have been reported for either **1** or **2**.

Scheme 1

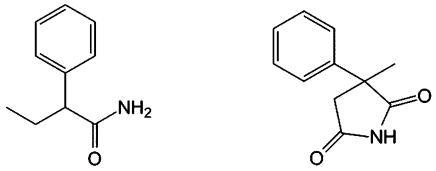

1 **2**

The main goal of the presented project was a detailed characterization of all racemic and enantiomeric forms of mentioned compounds with the single crystal X-ray diffraction method and discussion of the relationship of their molecular and crystal structure to the physicochemical properties of different forms of compounds **1** and **2**. The following notations are used for the studied compounds: 2-phenylbutyramide **1**, α-methyl-α-phenylsuccinimide **2**, their racemic forms are called *rac*-**1** and *rac*-**2**; after racemic forms have been separated we call them in accordance with an order of eluted fractions **1a** and **2a**, and **1b** and **2b**, respectively. The enantiomeric forms characterized with X-ray analysis in accordance with their stereochemistry are called *R* or *S*, and in accordance with their optical activity are called + (plus) or − (minus). In the case of a polymorphic compound a name of singony was added to the corresponding notation.

MATERIALS AND METHODS

Chemicals. 2-Phenylbutyramide and α-methyl-α-phenylsuccinimide (3-methyl-3-phenylpyrrolidine-2,5-dione) were purchased from Alfa Aesar and Sigma-Aldrich, respectively. Acetonitrile and methanol (Omnisolv, gradient grade), hexanes, and acetone were obtained from

Table 1. Crystallographic Data for Compound 1

compound	*rac*-**1**	(*R*)-**1**	(*S*)-**1**
empirical formula	$C_{10}H_{13}NO$	$C_{10}H_{13}NO$	$C_{10}H_{13}NO$
fw	163.21	163.21	163.21
radiation	Mo Kα	Cu Kα	Cu Kα
temperature (K)	100	100	100
cryst size (mm)	0.30 × 0.18 × 0.15	0.44 × 0.10 × 0.08	0.28 × 0.24 × 0.04
cryst syst	monoclinic	triclinic	triclinic
space group	*C*2/*c*	*P*1	*P*1
a (Å)	24.197(2)	5.1916(1)	5.1941(1)
b (Å)	5.1143(3)	9.4525(2)	9.4531(1)
c (Å)	17.669(1)	10.0367(2)	10.0232(1)
α (deg)	90	96.326(1)	96.343(1)
β (deg)	121.267(1)	102.938(1)	102.945(1)
γ (deg)	90	104.998(1)	104.938(1)
V (Å^3)	1869.0(2)	456.23(2)	455.97(1)
Z	8	2	2
d_c (g cm^{-3})	1.160	1.188	1.189
F(000)	704	176	176
μ (mm^{-1})	0.075	0.607	0.607
θ range (deg)	1.97−30.00	4.59−69.99	4.60−70.00
index range	$-33 \le h \le 34$	$-6 \le h \le 6$	$-6 \le h \le 6$
	$-7 \le k \le 7$	$-11 \le k \le 11$	$-11 \le k \le 11$
	$-24 \le l \le 24$	$-10 \le l \le 12$	$-12 \le l \le 12$
reflections collected	11537	11121	10827
reflections unique/R_{int}	2717/0.026	3010/0.038	2980/0.022
reflections with $I > 2\sigma(I)$	2181	2991	2955
R_1/wR_2 ($I > 2\sigma(I)$)	0.0412/0.1123	0.0321/0.0815	0.0288/0.0750
R_1/wR_2 (all data)	0.0530/0.1185	0.0323/0.0818	0.0290/0.0755
data/parameters	2717/116	3010/231	2980/231
GOF on F^2	1.001	1.000	1.001
Flack/Hooft parameters	not appl	0.24(19)/—	0.09(18)/—
no. of Bijvoet pairs		1315 (76%)	1286 (74%)
largest diff peak/hole (e·Å^{-3})	0.356/−0.185	0.121/−0.171	0.172/−0.175
abs cor T_{max}; T_{min}	0.989; 0.978	0.953; 0.776	0.976; 0.848

dx.doi.org/10.1021/cg500284q | *Cryst. Growth Des.* 2014, 14, 3360−3369

Table 2. Crystallographic Data for Compound 2

compound	*rac*-**2**	(*R*)-**2m**	(*S*)-**2m**	(*R*)-**2o**	(*S*)-**2o**
empirical formula	$C_{11}H_{11}NO_2$	$C_{11}H_{11}NO_2$	$C_{11}H_{11}NO_2$	$C_{11}H_{11}NO_2$	$C_{11}H_{11}NO_2$
fw	189.21	189.21	189.21	189.21	189.21
radiation	Mo Kα	Cu Kα	Cu Kα	Cu Kα	Cu Kα
temperature (K)	296	100	100	100	100
cryst size (mm)	0.30 × 0.20 × 0.20	0.30 × 0.25 × 0.20	0.30 × 0.20 × 0.20	0.30 × 0.24 × 0.21	0.35 × 0.30 × 0.25
cryst syst	monoclinic	monoclinic	monoclinic	orthorhombic	orthorhombic
space group	$P2_1/c$	$P2_1$	$P2_1$	$P2_12_12_1$	$P2_12_12_1$
a (Å)	7.3699(9)	6.70721(7)	6.7076(5)	6.7078(1)	6.7089(1)
b (Å)	22.592(3)	7.01427(7)	7.0112(5)	7.1693(1)	7.1714(1)
c (Å)	11.7988(15)	10.0182(1)	10.0210(7)	19.0492(3)	19.0480(2)
α (deg)	90	90	90	90	90
β (deg)	90.308(2)	102.6398(3)	102.635(2)	90	90
γ (deg)	90	90	90	90	90
V (Å^3)	1964.5(4)	459.895(9)	459.86(6)	916.08(2)	916.44(2)
Z	8	2	2	4	4
d_c (g cm^{-3})	1.280	1.366	1.366	1.372	1.371
F(000)	800	200	200	400	400
μ (mm^{-1})	0.089	0.773	0.773	0.776	0.776
θ range (deg)	0.90−30.00	4.52−72.12	4.52−69.94	4.64−71.98	4.64−71.95
index range	$-10 \le h \le 10$	$-8 \le h \le 8$	$-8 \le h \le 7$	$-8 \le h \le 8$	$-7 \le h \le 8$
	$-31 \le k \le 31$	$-8 \le k \le 6$	$-8 \le k \le 8$	$-8 \le k \le 8$	$-8 \le k \le 8$
	$-16 \le l \le 16$	$-12 \le l \le 12$	$-12 \le l \le 12$	$-23 \le l \le 23$	$-23 \le l \le 23$
reflections collected	25061	8828	13074	16767	22269
reflections unique/R_{int}	5725/0.022	1631/0.024	1696/0.035	1793/0.035	1797/0.027
reflections with $I > 2\sigma(I)$	4559	1631	1696	1792	1795
R_1/wR_2 ($I > 2\sigma(I)$)	0.0490/0.1314	0.0266/0.0686	0.0257/0.0688	0.0258/0.0647	0.0249/0.0624
R_1/wR_2 (all data)	0.0637/0.1406	0.0266/0.0686	0.0257/0.0688	0.0258/0.0647	0.0250/0.0624
data/parameters	5725/256	1631/132	1696/132	1793/132	1797/132
GOF on F^2	1.002	1.006	1.002	1.002	1.002
Flack/Hooft parameters	not appl	0.00(19)/0.07(4)	0.17(18)/0.11(4)	0.06(20)/0.01(4)	0.05(19)/0.05(2)
No. of Bijvoet pairs		663 (80%)	754 (95%)	718 (99%)	719 (99%)
largest diff peak/hole (e·Å^{-3})	0.251/−0.210	0.195/−0.137	0.187/−0.130	0.188/−0.141	0.186/−0.134
abs cor T_{max}; T_{min}	0.982; 0.974	0.861; 0.801	0.861; 0.801	0.854; 0.801	0.830; 0.773

EM Science. Ultrapure (18.2 MOhm) water was produced in-house using Barnstead NANOpure Diamond system (Thermo Scientific).

Chiral Liquid Chromatography. Resolution of enantiomers of **1** and **2** was performed by chiral high-performance liquid chromatography (HPLC) in reversed phase mode. Briefly, enantiomers of **1** were separated on Chiracel OD stationary phase, and enantiomers of **2** on Chiracel OJ stationary phase (both from Daicel Chemical Industries, Ltd.) using gradients of MeOH in H_2O. Collected fractions were dried *in vacuo* to give powder materials used in the experiments described in this paper. On the basis of analytical chiral HPLC, the enantiomeric purify of enantiomers of **1** thus prepared was 93−95%, and enantiomeric purity of enantiomers of **2**, due to the better resolution achieved in preparative chromatography, was 96−98%.

X-ray Single Crystal Structure Analysis. Data were collected on a Bruker APEX-II CCD diffractometer (graphite monochromator, ω and φ scan mode) and corrected for absorption.[13] For details of experiments and structure solution, see Tables 1 and 2. The structures were determined by direct methods and refined by a full-matrix least-squares technique on F^2 with the anisotropic displacement parameters for non-hydrogen atoms. For the enantiomers of **2**, the absolute configurations were reliably determined by the refinement of Flack parameters[14] and confirmed by calculations of Hooft parameters[15] (Tables 1 and 2). For (*R*)-**1** and (*S*)-**1**, it was impossible to calculate the Hooft parameters because of an insufficient number of the measured Friedel pairs, and thus only the Flack parameters were used. The hydrogen atoms of the amino groups were localized in the difference Fourier maps and included into refinement with fixed isotropic displacement parameters (U_{iso}(H) = 1.2U_{eq}(N)), except for compound *rac*-**2**, in which the positional parameters of these atoms were also fixed. The other hydrogen atoms were placed in calculated positions and refined in riding model with fixed isotropic displacement parameters (U_{iso}(H) = 1.5U_{eq}(C) for the CH_3-groups and U_{iso}(H) = 1.2U_{eq}(C) for the other groups). All calculations were carried out by use of the SHELXTL program package.[16] Crystallographic data have been deposited with the Cambridge Crystallographic Data Center, CCDC 938765−938772. Copies of this information may be obtained free of charge from the Director, CCDC, 12 Union Road, Cambridge CB2 1EZ, UK (Fax: +44 1223 336033; e-mail: deposit@ccdc.cam.ac.uk or www.ccdc.cam.ac.uk).

IR Spectroscopy, CD Spectroscopy, and Melting Point Determination. Powder infrared (IR) spectra of finely grounded crystals were recorded in attenuated total reflection (ATR) mode at room temperature (22 °C) on Magna-IR 550 FT-IR spectrometer (Thermo Nicolet) with the Linear Baseline Correction.

Far-UV (200−280 nm) circular dichroism (CD) spectra of 1-mM solutions of **1** and **2** in AcCN/H_2O (1:1) were recorded on a model 420 CD spectrometer (Aviv Biomedical, Lakewood, NJ) in a 0.1 cm path length quartz optical cell. A 2 nm spectral bandwidth was used, and three or five scans were collected and averaged for each sample. The optical bench was purged with dry N_2.

Melting points were measured on OptiMelt automated melting point system (Stanford Research Systems Ltd.) controlled by MeltView software version V.1.107. Heating rate of 1 °C/min was used, and the detection thresholds were set as follows: 10% for clear point, 50% for single (meniscus) point, and 70% for onset point.

dx.doi.org/10.1021/cg500284q | *Cryst. Growth Des.* 2014, 14, 3360−3369

RESULTS AND DISCUSSION

Chromatographic Resolution, Relative Configuration, and Crystallization of 1 and 2. Enantiomers of compounds **1** and **2** were resolved by chiral reversed phase HPLC (see Materials and Methods). Far-UV CD spectra of enantiomers of **1** (Figure 1a) show a positive Cotton effect around 225 nm for

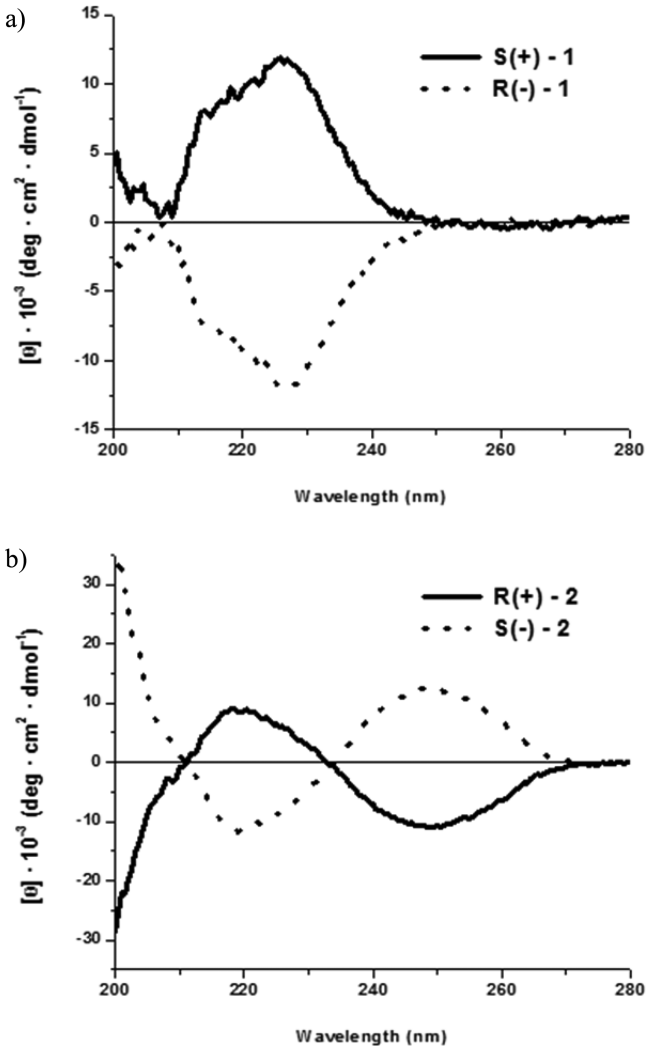

Figure 1. Far-UV CD spectra of enantiomers of **1** (a) and **2** (b) in AcCN/H_2O (1:1).

the enantiomer that elutes first, and a negative Cotton effect for the enantiomer that elutes second. Far-UV CD spectra of enantiomers of **2** (Figure 1b) are more complex: the enantiomer that elutes first has a positive Cotton effect around 220 nm and a negative one around 250 nm, while the enantiomer that elutes second has opposite signs of the Cotton effects. Thus, for both compounds (+) enantiomers elute first, and (−) enantiomers second. This is in accordance with our polarimetry data. Far-UV (200−300 nm) CD spectrum of (−)-**2** in AcCN/H_2O (1:1) (Figure 1b) closely resembles the far-UV (210−280 nm) spectrum of this enantiomer in MeOH previously reported by Knabe and Koch.[17]

After trying several different crystallization conditions, we found that crystals of racemic and homochiral forms of **1** and **2** grown from either 40 mg/mL solutions in AcCN/H_2O (1:1) at 4 °C or 15 mg/mL solutions in hexanes/acetone (2:1) at 22 °C are of a quality well suitable for single-crystal X-ray diffraction crystallography.

MOLECULAR AND CRYSTAL STRUCTURES

The structures of both racemic and enantiomerically pure compounds **1** and **2** obtained by chiral chromatography separations have been investigated by X-ray diffraction analysis. The absolute configurations of enantiomers have been established based on the anomalous dispersion effects observed with Cu Kα radiation. Because the presence of only one or two oxygen atoms in compounds **1** and **2**, we have carried out the experimental X-ray diffraction studies for both enantiomers of each compound to get more indicative values of Flack parameters. Evidently, the structures of (*R*)- and (*S*)-enantiomers of the same compound are mirror images of each other. Therefore, only (*R*)-enantiomers of **1** and **2** are described below (for full X-ray data of the (*S*)-enantiomers of **1** and **2**, see Supporting Information).

The molecular structures of (*R*)-**1** and *rac*-**1** are shown in Figure 2 along with the atomic numbering schemes. Enantiomer (*R*)-**1** crystallizes in the triclinic space group *P*1 with the two crystallographically independent molecules

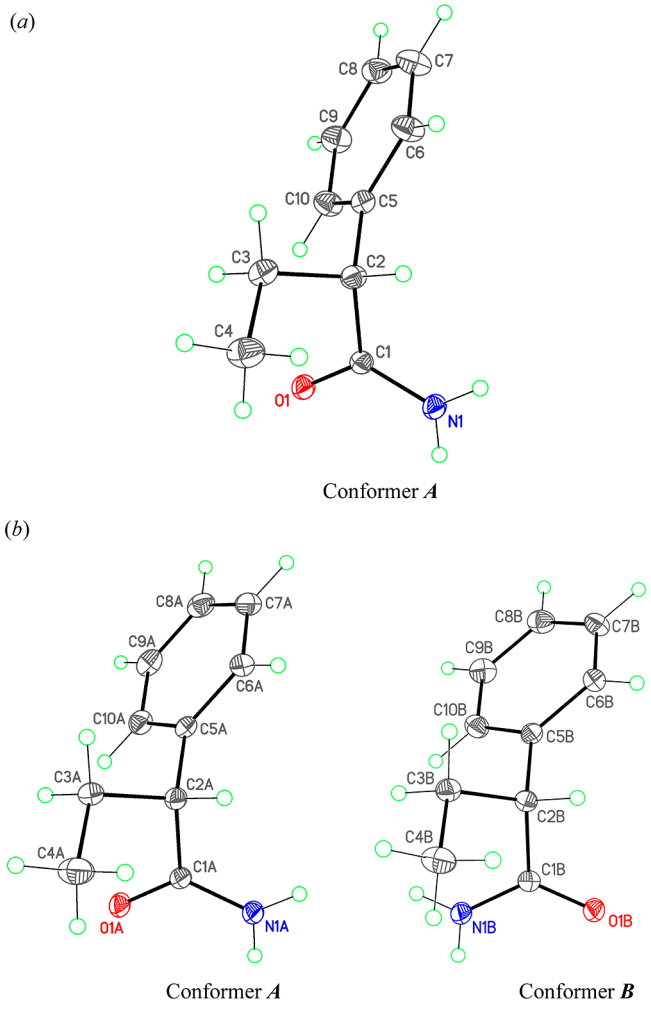

Figure 2. Molecular structures of (*a*) *rac*-**1** (conformer A) and (*b*) (*R*)-**1** (the two crystallographically independent molecules—conformers **A** and **B** distinguishing by rotation of the 1-phenylpropyl substituent about the C1−C2 bond).

dx.doi.org/10.1021/cg500284q | *Cryst. Growth Des.* 2014, 14, 3360−3369

representing different conformers **A** and **B** (Figure 1b). The conformers **A** and **B** are distinguished by rotation of the amide group around the C1−C2 bond (the N1−C1−C2−C3 torsion angles are 32.26(18) and −144.08(13)°, in conformers **A** and **B** respectively). A superposition of two conformers shown in Figure 3 demonstrates significant difference between them

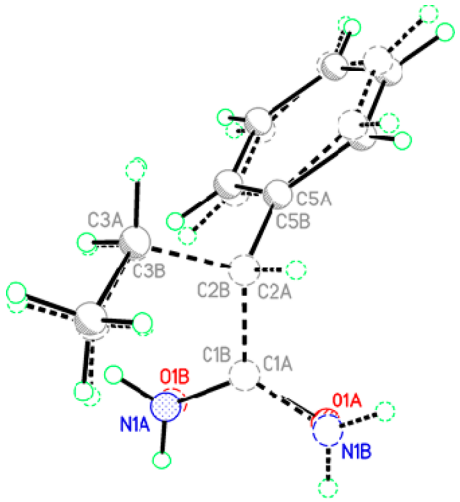

Figure 3. Superposition of conformers **A** and **B** in enantiomeric form (*R*)-**1**.

attributed to rotation of amide group by ∼180° around the C1−C2 bond. Unlike (*R*)-**1**, *rac*-**1** crystallizes in the monoclinic space group *C*2/*c* and consists of the only A conformers (the N1−C1−C2−C3 torsion angle is −130.06(9)°). The geometrical parameters of molecules (*R*)-**1** and *rac*-**1** are very similar and are in good agreement with those found in the literature.

The molecule of **1** contains one hydrogen-bond acceptor and two donor sites. In order to satisfy condition of H-bonds formation by all potential hydrogen-bonding acceptors and donors, each carbonyl group should act as a bifurcated hydrogen-bond acceptor, and both hydrogen atoms of each amide groups should act as hydrogen-bond donors. As a result, the molecules (*R*)-**1** and *rac*-**1** produce very similar crystal structures despite the differences in molecular structures. The presence of two conformers in (*R*)-**1** also helps to satisfy this condition. Thus, in the crystals of both (*R*)-**1** and *rac*-**1**, there are the infinite ribbons built via the N−H···O hydrogen bonds (Figure 4, Table 3). The ribbons in (*R*)-**1** are chiral and are composed of both conformers **A** and **B** (Figure 4b), whereas the ribbons in *rac*-**1** are centrosymmetric (Figure 4a). The amide groups within the chains are practically coplanar, and the bulk phenyl substituents are arranged in anti-position relative to the acetamide fragment plane. The infinite ribbons are further packed in similar *parquet* pattern in both (*R*)-**1** and *rac*-**1** structures (Figure 5). It is interesting to note that the analogous H-bonded ribbons are also formed in the crystals of other related amides.[18,19] Similarity of hydrogen bonds characteristics and molecular packings for (*R*)-**1** and *rac*-**1** suggests that their physicochemical properties might be similar as well. This is supported by the close similarity of IR spectral characteristics of racemic and enantiomeric forms and by very close values of melting points for all forms of **1**.

Crystallographic studies revealed that enantiomers of **2** form two different polymorphs when crystallized from different solvents (Table 2). Crystallization of **2** from AcCN/H_2O (1:1) gives monoclinic form (**2m**, space group $P2_1$), while its crystallization from hexanes/acetone (2:1) gives orthorhombic form (**2o**, space group $P2_12_12_1$). The crystal shape of two polymorphs is presented in Figure 6. *rac*-**2** crystallizes from hexane/acetone and acetone/water solution in the monoclinic space group $P2_1/c$ with the two crystallographically independent molecules.

The molecular structures of (*R*)-**2** and *rac*-**2** are shown in Figure 7 along with the atomic numbering schemes. The geometrical parameters of molecules (*R*)-**2m**, (*R*)-**2o**, and *rac*-**2** are very close to each other and comparable to those found for the related compounds.[20−26] Superposition of molecules **2** from monoclinic and orthorhombic polymorphs (Figure 8) shows close molecular similarity in these forms.

In contrast to **1**, the molecule **2** contains two hydrogen-bond acceptor and one donor sites. As a result, in the crystal, the succinimides usually form either dimers[20,26] or infinite chains[21−25] by hydrogen bonding between the imide hydrogen atom and carbonyl oxygen atom of adjacent molecules. In the case of **2**, the molecules both in the enantiomerically pure **2m** and **2o** and in the racemate *rac*-**2** are linked by the intermolecular N1−H1···O2 hydrogen bonds (Table 3) into one-dimensional *zigzag*-like chains running in the *b* and *a* directions, respectively (Figure 9, left). The fact that only O2 oxygen atom acts as a protonoacceptor is apparently explained by the steric reasons. The succinimide rings within the chains are almost coplanar. Nevertheless, despite the obvious similarity of these chains, there is a striking distinction between them, namely, *anti* (in the enantiomerically pure **2m** and **2o**), similar to **1**, and *syn* (in the racemic *rac*-**2**), unlike **1**, mutual disposition of the phenyl substituents relative to the succinimide ring plane (Figure 9, right). It should be noted that, to the best our knowledge, the less sterically favorable *syn* configuration of the phenyl rings within the H-bonded chains is observed for the first time among compounds of this type.[27] The main structural motifs the H-bonded *zigzag*-like chains in the two polymorphs **2m** and **2o** are quasi-identical. The crystal structures of these polymorphs are characterized by the different packing of the H-bonded chains. In the crystal structure of **2o**, the H-bonded chains are packed congruently, i.e., without changing of the conformations relative to each other (Figure 9a, right), while, in the crystal structure of **2m**, these chains are packed incongruently, with rotation by 180 deg in turn along the *c* axis (Figure 9b, right). Due to the *syn*-configuration of the phenyl rings, the crystal packing of the H-bonded chains in *rac*-**2** is *zipper*-like (Figure 9c).

Solid-State IR Spectroscopy of Racemic and Homochiral Forms of 1 and 2. No substantial differences were observed in powder IR spectra between racemic and homochiral forms of **1**. However, a powder IR spectrum of racemic form of **2** is different from spectra of homochiral forms of this compound in the N−H stretch region (Figure 10).

It appears that spectral data are closely related to distinctions of supramolecular organization in racemate−enantiomer and polymorphs pairs. For compound **1**, the presence of two conformers in enantiomeric crystal allows the racemic H-bonded chain to be closely mimicked, which leads to very close similarity of solid state IR spectra for *rac*-**1**, *R*-**1** and *S*-**1**. On the contrary, dissimilarity of supramolecular organization for *rac*-**2** and both polymorphs of **2** (H-bonded molecular chains with *transoid* orientation for enantiomeric polymorphs and with *cisoid* orientation for racemate) leads to differences in

dx.doi.org/10.1021/cg500284q | *Cryst. Growth Des.* 2014, 14, 3360−3369

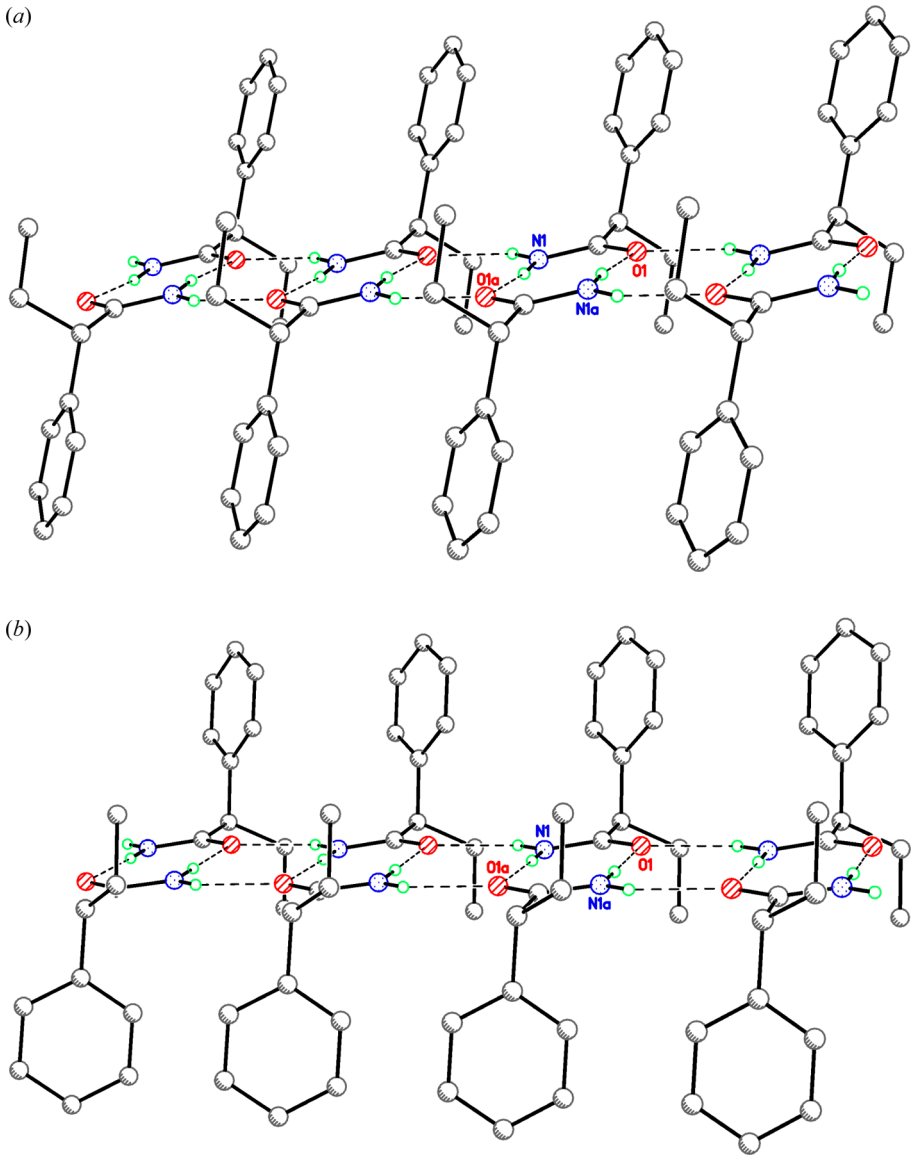

Figure 4. Infinite H-bonded ribbons in (a) *rac*-**1** (centrosymmetric) and (b) (*R*)-**1** (chiral).

Table 3. Intermolecular N−H···O Hydrogen Bonds (Å and deg) in 1 and 2

D[a]−H···A[a]	*d*(D−H)	*d*(H···A)	*d*(D···A)	∠(D−H···A)
rac-**1**				
N1−H1A···O1 [*x*, −1+*y*, *z*]	0.888(16)	2.067(15)	2.8797(11)	151.8(14)
N1−H1B···O1 [1/2−*x*, 3/2−*y*, 1−*z*]	0.896(19)	2.042(19)	2.9335(14)	173.2(13)
(*R*)-**1**				
N1−H1A···O1A	0.84(2)	2.05(2)	2.8882(16)	175(2)
N1−H1B···O1 [−1+*x*, *y*, *z*]	0.84(2)	2.19(2)	2.9591(16)	152(2)
N1A−H1C···O1A [1+*x*, *y*, *z*]	0.88(2)	2.16(2)	2.9497(15)	150(2)
N1A−H1D···O1	0.89(2)	2.07(2)	2.9581(17)	178(2)
rac-**2**				
N1A−H1A···O2B [*x*, *y*, −1+*z*]	0.86	1.97	2.823(2)	170
N1B−H1B···O2A [1+*x*, *y*, 1+*z*]	0.86	2.04	2.862(2)	160
(*R*)-**2m**				
N1−H1A···O2 [−*x*, −1/2+*y*, 2−*z*]	0.864(19)	1.961(16)	2.8241(15)	176(2)
(*R*)-**2o**				
N1−H1···O2 [−*x*, 1/2+*y*, 3/2−*z*]	0.916(14)	1.933(14)	2.8374(14)	168.99(14)

[a]D − proton donor, A − proton acceptor.

dx.doi.org/10.1021/cg500284q | *Cryst. Growth Des.* 2014, 14, 3360−3369

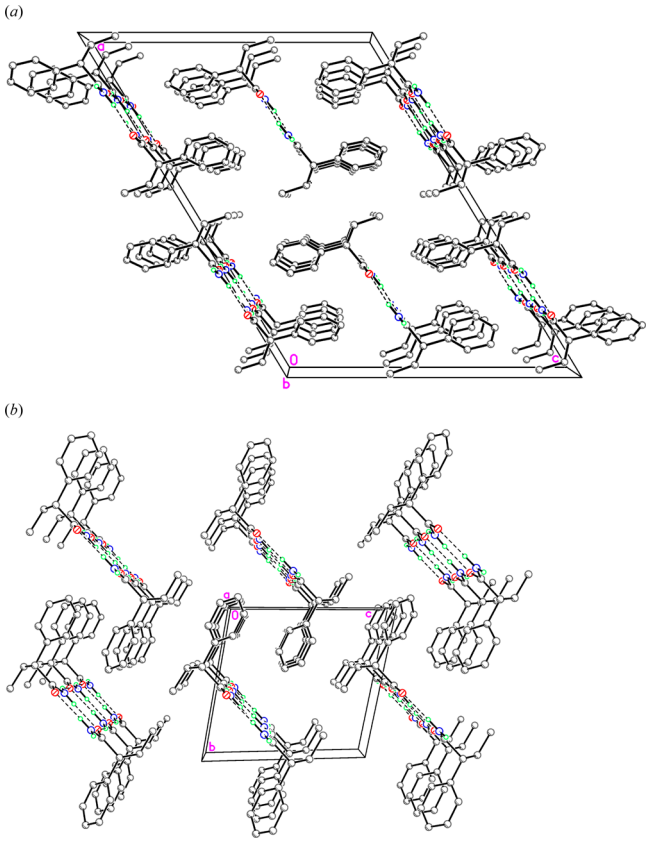

Figure 5. Crystal packing of the H-bonded ribbons in (a) *rac*-**1** (along the *b* axis) and (*b*) (*R*)-**1** (along the *a*-axis). The dashed lines indicate the intermolecular N−H···O hydrogen bonds.

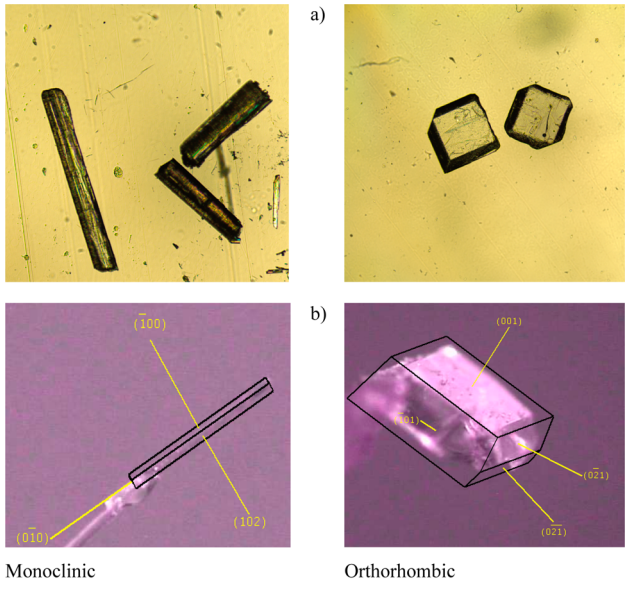

Figure 6. Crystal shape of two homochiral polymorphs of compound **2**. (a) Microscopic pictures of needle-like crystals (*R*)-**2m** (left) and prismatic (*R*)-**2o** (right); Miller indexes of crystal faces of forms (*R*)-**2m** (left) and (*R*)-**2o** (right).

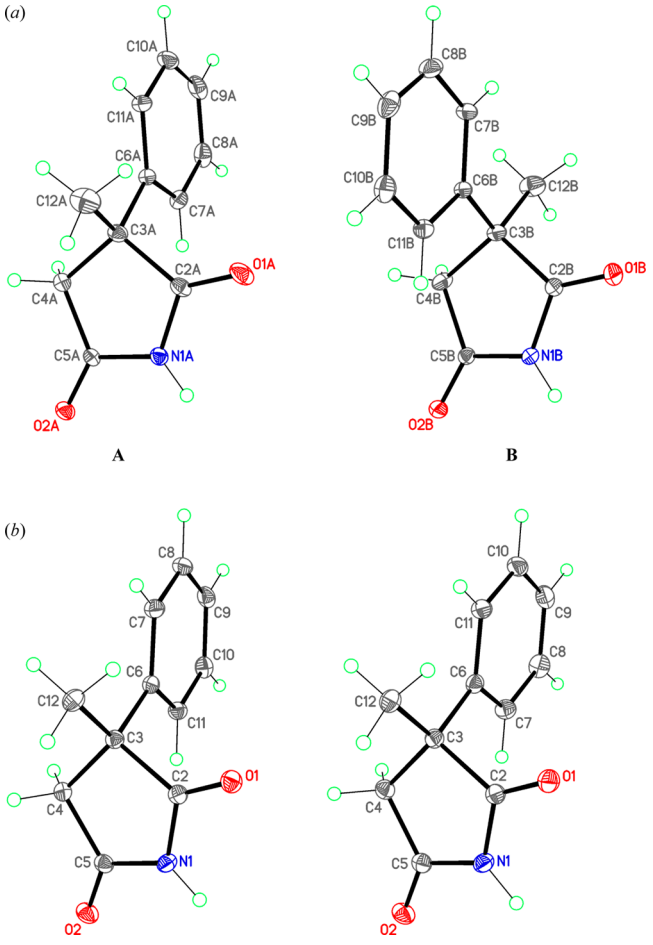

Figure 7. Molecular structures of (a) *rac*-**2** (the two crystallographically independent molecules representing the different enantiomers) and (b) (*R*)-**2m** (left) and (*R*)-**2o** (right).

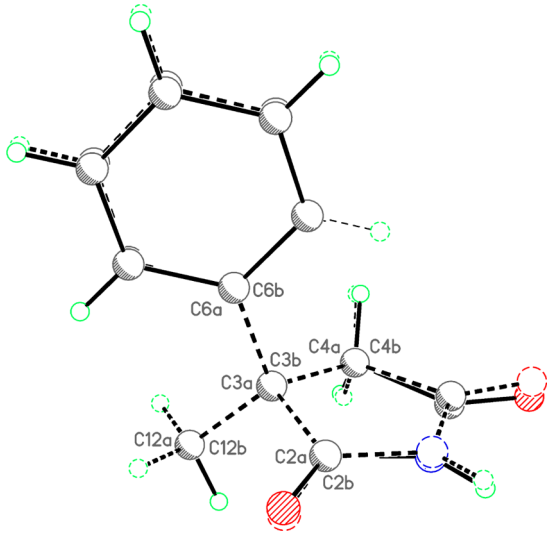

Figure 8. Superposition of molecules in monoclinic and orthorhombic polymorphs of (*R*)-**2**.

geometric characteristics of hydrogen bonding and crystal packing and, as a consequence, to different spectral characteristics (Figure 10, Table 4). Due to similarity of molecular packing in polymorphs of **2** (**2m** and **2o**), their spectral characteristics are also similar to small deviations related to slight differences in hydrogen bonding.

Crystal Density and Melting Points of Racemic and Homochiral Forms of 1 and 2. Usually denser compounds with tightly packed molecules are considered to be more

dx.doi.org/10.1021/cg500284q | *Cryst. Growth Des.* 2014, 14, 3360−3369

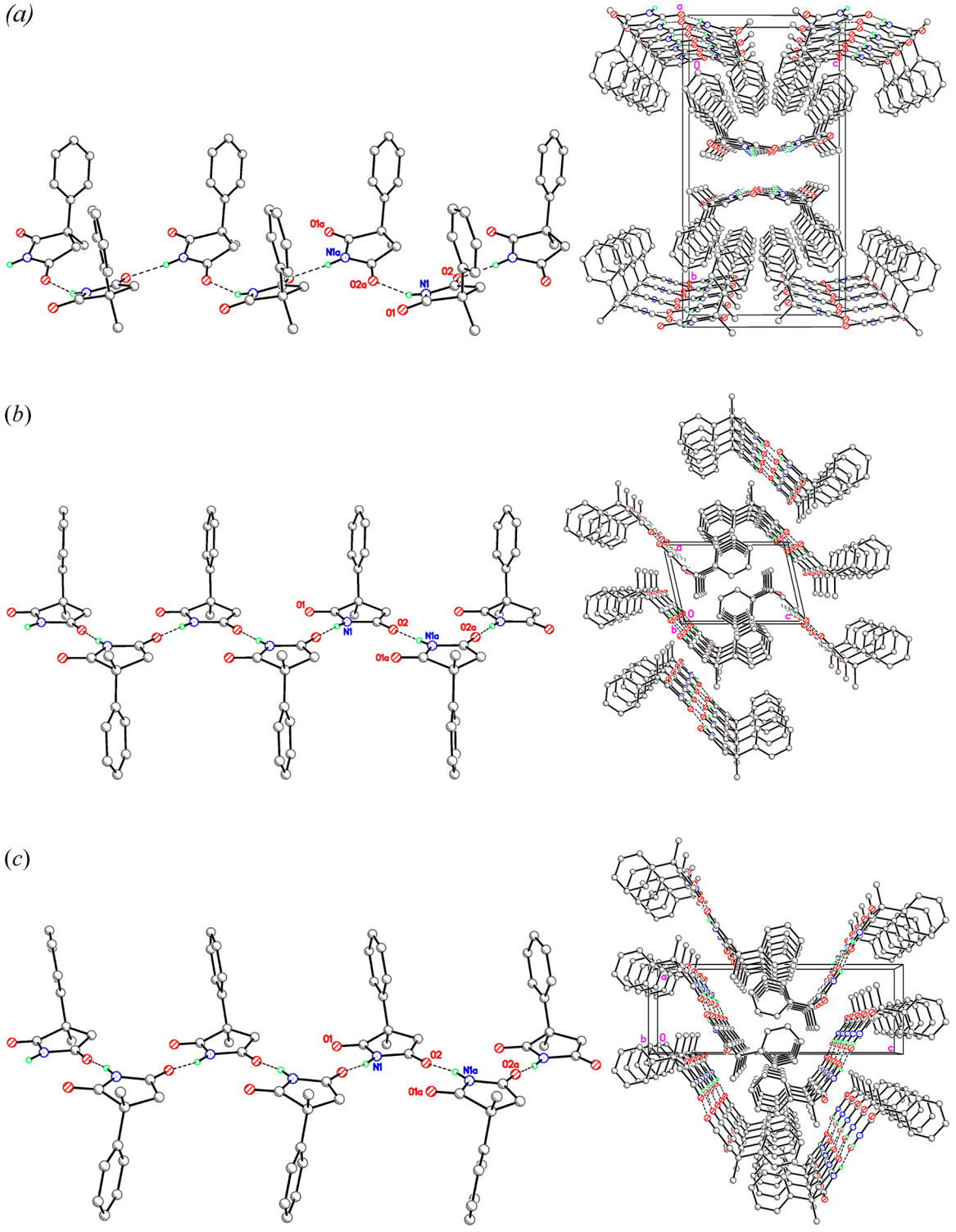

Figure 9. Infinite H-bonded chains (left) and their crystal packing (right) in (a) *rac*-**2**, (b) (*R*)-**2m**, and (c) (*R*)-**2o**. The dashed lines indicate the intermolecular N−H···O hydrogen bonds.

thermodynamically stable.[7] Comparison of eight pairs of homochiral and racemic compounds conducted by Wallach in 1895 allowed him to formulate a rule that racemic compounds have a trend to be denser than enantiomers.[28] Statistical analysis carried out by Brock at al.[29] based on CSD data in 1991 revealed that such trend in general exists for racemic crystals composed of enantiomers that can be resolved chemically. However, exceptions to this rule are described in the literature.[30,31] In contrast to the Wallach rule, compound **2**, unlike compound **1**, demonstrates a higher density of chiral crystals in comparison to its racemate (difference is ca. 0.1 g cm^{-3}, Table 2). That might be an indication that compound **2** in chiral forms is at least as stable as its racemate.

Interesting observations were obtained for melting points of studied materials. If for racemic and homochiral forms of **1** melting points are very close, for **2** melting points differ

dx.doi.org/10.1021/cg500284q | *Cryst. Growth Des.* 2014, 14, 3360−3369

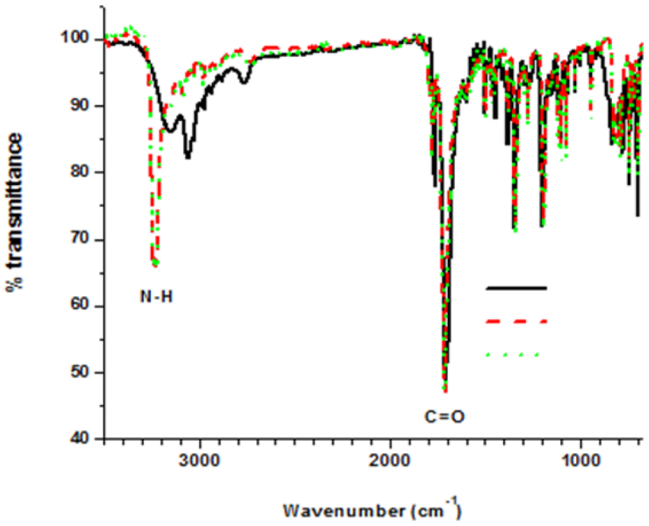

Figure 10. Solid-state IR spectra of racemic and homochiral forms of **2**. Black solid line *rac*-**2**, red dashed line *R*-(+)-**2o**, green dotted line *S*-(−)-**2o**. To facilitate the comparison, the spectra were normalized to the spectrum of racemate at their peak intensities in the C═O stretch (1708−1711 cm^{-1}) region.

Table 4. Melting Points for Racemic and Homochiral Compounds 1 and 2[a]

	onset point (°C)	single point (°C)	clear point (°C)
	Compound **1**		
rac-**1**	83.5 ± 0.09	83.9 ± 0.12	84.6 ± 0.05
(*R*)-**1**	80.4 ± 0.28	80.9 ± 0.25	81.7 ± 0.28
(*S*)-**1**	78.0 ± 0.35	79.5 ± 0.23	80.6 ± 0.22
	Compound **2**		
rac-**2**	81.6 ± 0.05	82.4 ± 0.24	83.9 ± 0.12
(*R*)-**2m**	115.0 ± 0.12	115.6 ± 0.23	116.3 ± 0.09
(*S*)-**2m**	114.8 ± 0.12	115.6 ± 0.23	116.2 ± 0.23
(*R*)-**2o**	114.1 ± 0.07	116.1 ± 0.03	117.3 ± 0.07
(*S*)-**2o**	114.2 ± 0.06	116.2 ± 0.03	117.2 ± 0.03

[a]For compound **2**, data for two polymorphs **2m** (monoclinic) and **2o** (orthorhombic) are presented.

significantly (Table 4). These results can be explained by the close similarity of molecular packings in all forms of **1** and by dissimilarities in supramolecular aggregates and molecular packings in crystals **2** (chains with *transoid* orientation for enantiomeric polymorphs and with uncommon *cisoid* orientation for racemate). For racemate **2**, lower crystal density and lower melting temperature (difference ∼33°) suggest its lower stability.

CONCLUSIONS

Enantiomers of compounds **1** and **2** were separated by chiral chromatography, and their absolute configurations were reliably established by analysis of anomalous X-ray scattering using refinement of Flack and Hooft parameters. A combination of X-ray and CD data allowed the following designations for the enantiomers: *R*-(−)-**1**, *S*-(+)-**1**, *R*-(+)-**2**, *S*-(−)-**2**. The assignments for **2** are in accordance with the study by Knabe and Koch,[17] who determined relative and absolute configurations of enantiomers of this compound by establishing a correlation between their optical activity and optical activity of their synthetic precursors of known absolute configuration. In crystals of racemate and enantiomers of **1**, the robust molecular synthons with very similar structure and hydrogen bonding pattern were found. The existence of such synthons in the enantiomers was due to the presence of two molecular conformations that allowed mimicking of molecular hydrogen bonded chains found in the racemate. Structural similarity of racemate and homochiral forms for **1** and polymorphs for **2** explains the close similarity of their IR spectra and melting points. On the basis of presented structural characteristics, it is possible to speculate that bioactivity for all forms of **1** will be similar, while for **2** it might be different.

ASSOCIATED CONTENT

Supporting Information

Crystallographic information file. This material is available free of charge via the Internet at http://pubs.acs.org.

AUTHOR INFORMATION

Corresponding Authors

*(T.V.T.) E-mail: tvtimofeeva@nmhu.edu.
*(A.V.K.) E-mail: arcadius.krivoshein@acphs.edu.

Notes

The authors declare no competing financial interest.

ACKNOWLEDGMENTS

Funding from the U.S. National Science Foundation (projects PREM DMR-0934212 and IIA-1301346) and Russian Foundation for Basic Research (11-03-00652 (V.N.K.)) is gratefully acknowledged.

REFERENCES

(1) (a) Lenz, W. *Deutsch Med. Wschr.* **1961**, *86*, 2555−2556. (b) Lenz, W.; Pfeiffer, R. A.; Kosenow, W.; Hayman, D. J. *Lancet* **1962**, *279*, 45−46.
(2) McBride, W. G. *Lancet* **1961**, *278*, 1358−1360.
(3) Botting, J. *Drug News Perspect.* **2002**, *15*, 604−611.
(4) Blaschke, G.; Kraft, H. P.; Fickentscher, K.; Kohler, F. *Arzneimittelforschung* **1979**, *29*, 1640−1642.
(5) Eriksson, T.; Björkman, S.; Roth, B.; Fyge, Å.; Höglund, P. *Chirality* **1995**, *7*, 44−52.
(6) Nunez, M. C.; Garcia-Rubino, M. E.; Conejo-Garcia, A.; Cruz-Lopez, O.; Kimatrai, M.; Gallo, M. A.; Espinosa, A.; Campos, J. M. *Current Med. Chem.* **2009**, *16*, 2064−2074.
(7) Reddy, I. K.; Mehvar, R., Eds. *Chirality in Drug Design and Development*; Taylor & Francis: New York, 2004; p 393.
(8) (a) Krivoshein, A. V.; Poreddy, A. R.; Covey, D. F.; Hess, G. P. *Soc. Neurosci. Abstracts* **2006**, *523*, 9/C56. (b) Krivoshein, A. V. *Biochem. J.* **2014**, submitted.
(9) Porter, R. J.; Penry, J. K.; Lacy, J. R.; Newmark, M. E.; Kupferberg, H. J. *Neurology* **1979**, *29*, 1509−1513.
(10) Browne, T. R.; Feldman, R. G.; Buchanan, R. A.; Allen, N. C.; Fawcett-Vickers, L.; Szabo, G. K.; Mattson, G. F.; Norman, S. E.; Greenblatt, D. J. *Neurology* **1983**, *33*, 414−418.
(11) Sigler, M.; Strassburg, H. M.; Boenigk, H. E. *Seizure* **2001**, *11*, 120−124.
(12) (a) Krivoshein, A. V., Chen, Y., and Torres, J. A. 17th IUPAB International Biophysics Congress, October 30−November 3, 2011, Beijing, China. (b) Krivoshein, A. V.; Bentum, S.; Chen, Y.; Torres, J. A.; Sandhu, B. K.; Timofeeva, T. V. *J. Pharm. Sci.* **2014**, submitted.
(13) Sheldrick, G. M. *SADABS, Bruker/Siemens Area Detector Absorption Correction Program*, v. 2.03; Bruker AXS: Madison, WI, 2003.
(14) (a) Flack, H. D. *Acta Crystallogr. A* **1983**, *39*, 876−881. (b) Flack, H. D.; Bernardinelli, G. *Acta Crystallogr. A* **2008**, *64*, 484−493. (c) Flack, H. D. *Acta Crystallogr. C* **2013**, *69*, 803−807.

(15) Hooft, R. W. W.; Straver, L. H.; Spek, A. L. *J. Appl. Crystallogr.* **2008**, *41*, 96−103.
(16) Sheldrick, G. M. *Acta Crystallogr.* **2008**, *64*, 112−122.
(17) Knabe, J.; Koch, W. *Arch. Pharm. (Weinheim)* **1972**, *305*, 849−854.
(18) Cohen-Addad, C. *Acta Crystallogr. B* **1979**, *35*, 2471−2472.
(19) Nichol, G. S.; Clegg, W. *Acta Crystallogr. C* **2011**, *67*, o13−o17.
(20) Argay, G.; Kálmán, A. *Acta Crystallogr. B* **1973**, *29*, 636−638.
(21) Karapetyan, A. A.; Andrianov, V. G.; Struchkov, Yu.T. *Cryst. Struct. Commun.* **1980**, *9*, 417−420.
(22) Alper, H.; Mahatantila, C. P. *Acta Crystallogr. C* **1985**, *41*, 548−550.
(23) Kwiatkowski, W.; Karolak-Wojciechowska, J. *Acta Crystallogr. C* **1992**, *48*, 204−206.
(24) Kwiatkowski, W.; Karolak-Wojciechowska, J. *Acta Crystallogr. C* **1992**, *48*, 206−208.
(25) Argay, G.; Fábián, L.; Kálmán, A. *Croat. Chem. Acta* **1999**, *72*, 551−565.
(26) Chong, S. Y.; Tremayne, M. *Chem. Commun.* **2006**, 4078−4080.
(27) Cambridge Structural Database, Release 2013, Cambridge, UK.
(28) Wallach, O. *Liebigs Ann. Chem.* **1895**, *286*, 90−143.
(29) Brock, C. P.; Schweizer, W. B.; Dunitz, J. D. *J. Am. Chem. Soc.* **1991**, *113*, 9811−9820.
(30) Patrick, B. O.; Brock, C. P. *Acta Crystallogr. B* **2006**, *62*, 488−497.
(31) Amharar, Y.; Petit, S.; Sanselme, M.; Cartigny, Y.; Petit, M.-N.; Coquerel, G. *Cryst. Growth Des.* **2007**, *7*, 1599−1607.